AIAA Journal
Vol. 43, No. 11, November 2005

Minimization of Acoustic Radiation from Thick Multilayered Sandwich Beams

H. Denli,* J. Q. Sun,† and T. W. Chou‡
University of Delaware, Newark, Delaware 19716

A study is presented of structural-acoustic optimizations of multilayered sandwich beams for minimal sound radiation. A sublaminate modeling approach of multilayered structures with a proper balance of accuracy and computational efficiency is adopted in this work. Finite elements are used to compute the vibration response and acoustic radiation of the structure. The material and geometric properties of an anisotropic sandwich beam are treated as design parameters. The objective of optimization is to minimize the acoustic power radiated by the structure. A piecewise objective function is studied that inherently includes nonlinear constraints of the optimization problem by taking advantages of the pattern search algorithm. Numerical examples are presented to show the effectiveness of the structural-acoustic optimization for the reduction of the radiated sound power.

Introduction

MULTILAYERED sandwich structures are widely used in the aerospace industry. These structures can be tailored to optimally achieve certain objectives. Our objective is to minimize the acoustic power radiated by the structure. This is accomplished by optimizing the structure with respect to a set of material or geometrical parameters. Optimizing material and geometric properties has become practically feasible because of the advances in composite manufacturing technologies and in numerical methods.

Minimization of structural sound radiation with respect to the geometry of beams and plates has been studied by Belegundu et al.,[1] Koopmann and Fahnline,[2] and Tinnsten.[3] Thamburaj and Sun have studied optimization problems of sound transmission loss with respect to geometric and anisotropic material parameters of sandwich beams.[4,5] Cunefare[6] and Naghshineh et al.[7] have developed an inverse approach to design structures that radiate sound inefficiently. The inverse approach proposes to first develop surface velocity profiles with minimum acoustic radiation known as "weak radiators"[8] and then optimize the structure with respect to a set of structural design parameters to meet the desired velocity profiles.

Structural modeling of thick laminated structures is a key step in optimization studies. The model needs to be computationally efficient and sufficiently accurate to describe the interlaminate dynamics of the multilayered structure. Many structural models have been proposed in the literature and can be found in the review articles.[9,10] A class of models in which we are interested has been reviewed by Noor et al.[11] and Reddy.[12] These models originally developed for thick laminated structures consist of a combination of fully and partially layerwise models and variable kinetic theories.

In this work, an optimization of multilayered sandwich structures for minimal sound radiation is studied. First, we present a layerwise theory with sublaminate approach to model the multilayered beam and derive the equations of motion of the structure under harmonic excitations by using finite elements. Next, we obtain the acoustic power radiated from the structure by using the Rayleigh integral leading to a quadratic form in terms of the normal velocities on the radiating surface of the sandwich. Finally, we study the optimization problem for minimizing the acoustic power with respect to a set of design parameters subject to the constraints. The optimization problem is solved by using a direct search optimization technique.[13] Numerical results are presented to demonstrate the theoretical development.

Structural-Acoustic Analysis

The analysis of thick laminated structures with anisotropic material discontinuity between laminates requires the determination of three-dimensional stress field.[14] However, direct three-dimensional modeling of the sandwich is computationally inefficient. Layerwise models have been proposed to improve the computational efficiency. Even though the layerwise theory is computationally more efficient than direct three-dimensional theories, the number of degrees of freedom in the layerwise theory still depends on the number of actual physical layers. A compromising solution for computational efficiency and accuracy is to use a sublaminate approach with layerwise modeling.[15] Each sublaminate contains a number of physical layers that are modeled by the sublaminate using the equivalent single-layer theory.

The layerwise theories have been extensively compared to the equivalent single-layer theories in terms of aspect ratio of beams and plates and elastic modulus ratio between adjacent anisotropic layers.[16,17] The studies suggest that for thick laminated beams with an aspect ratio 1/10 or greater and abrupt changes of elastic modulus between adjacent layers layerwise theories predict the natural frequencies of beams more accurately than the equivalent single-layer theories such as classical laminate theories, first and higher shear-order deformation theories. Because we consider thick multilayered sandwich beams with abrupt changes of elastic modulus between adjacent anisotropic layers, layerwise models combined with sublaminate approach are selected. Such a model represents a proper balance of accuracy and efficiency.

Consider a thick laminated sandwich beam as an example. The beam is split into several sublaminates, and each of them consists of a number of physical layers. We assume that the displacement fields of each sublaminate are expanded in power series of the thickness coordinate of the sublaminate

$$u^k(x, z^k) = \sum_{m=1}^{M} (z^k)^m u_m^k(x) \tag{1}$$

$$w^k(x, z^k) = \sum_{n=1}^{N} (z^k)^n w_n^k(x) \tag{2}$$

where k is an index of the sublaminate, z^k is the local thickness coordinate, m and n denote the order of local thickness coordinate,

Received 21 April 2005; revision received 28 June 2005; accepted for publication 28 June 2005.

*Graduate Student, Department of Mechanical Engineering.
†Professor, Department of Mechanical Engineering. Member AIAA.
‡Pierre S. du Pont Chair of Engineering, Department of Mechanical Engineering.

and $u_m^k(x)$ and $w_n^k(x)$ are the lateral and transverse displacements corresponding to the mth and nth orders of local thickness coordinates.

Based on these kinematic assumptions, we develop a finite element model of the multilayered beam. The elemental displacement field of the kth sublaminate can be expressed as a function of nodal displacements

$$\boldsymbol{w}_e^k = \begin{Bmatrix} u_e^k \\ w_e^k \end{Bmatrix} = \boldsymbol{Z}_M \boldsymbol{B}_M \boldsymbol{u}_e^k \tag{3}$$

where e refers to an element in the kth sublaminate, $\boldsymbol{Z}_M$ is the matrix only function of transverse local coordinate, $\boldsymbol{B}_M$ is the matrix only function of lateral local coordinates, and $\boldsymbol{u}_e^k$ is the nodal displacement vector of kth sublaminate.[18]

The infinitesimal strain-displacement relationship is

$$\begin{Bmatrix} (\gamma_{xx})_e^k \\ (\gamma_{zz})_e^k \\ (\gamma_{xz})_e^k \end{Bmatrix} = \begin{bmatrix} \dfrac{\partial}{\partial x} & 0 \\ 0 & \dfrac{\partial}{\partial z} \\ \dfrac{\partial}{\partial z} & \dfrac{\partial}{\partial x} \end{bmatrix} \boldsymbol{w}_e^k \qquad \text{or} \qquad \gamma_e^k = \boldsymbol{Z}_K \boldsymbol{B}_K \boldsymbol{u}_e^k \tag{4}$$

where $\boldsymbol{Z}_K$ and $\boldsymbol{B}_K$ are the matrices only functions of transverse and lateral coordinates respectively, which are obtained by reorganizing the derivatives of $\boldsymbol{Z}_M$ and $\boldsymbol{B}_M$ (Ref. 18).

In the lth physical layer of the kth sublaminate of the beam, the stresses can be computed from the constitutive relation as

$$\tau_e^l = \boldsymbol{Q}^l \gamma_e^k \tag{5}$$

where the elastic modulus matrix $\boldsymbol{Q}^l$ is given by

$$\boldsymbol{Q}^l = \begin{bmatrix} Q_{11}^l & Q_{12}^l & Q_{13}^l \\ & Q_{22}^l & Q_{23}^l \\ \text{sym} & & Q_{33}^l \end{bmatrix} \tag{6}$$

where subscripts 1 and 2 refer to the lateral and transverse directions. Q_{13} and Q_{23} are material constants that couple the normal stresses τ_{xx} and τ_{zz} to the shear strain γ_{xz}. The mass density matrix of the lth physical layer is given by

$$\boldsymbol{R}^l = \begin{bmatrix} \rho^l & 0 \\ 0 & \rho^l \end{bmatrix} \tag{7}$$

where ρ^l is the density of the lth physical layer. Thus, the element stiffness and mass matrices of the kth sublaminate can be expressed in element coordinates as

$$\boldsymbol{K}_e^k = b \int_{x_i}^{x_{i+1}} (\boldsymbol{B}_K)^T \left(\int_{h_{i-1}}^{h_i} \boldsymbol{Z}_K^T \boldsymbol{Q}^l \boldsymbol{Z}_K \,\mathrm{d}z \right) \boldsymbol{B}_K \,\mathrm{d}x$$

$$\boldsymbol{M}_e^k = b \int_{x_i}^{x_{i+1}} (\boldsymbol{B}_M)^T \left(\int_{h_{i-1}}^{h_i} \boldsymbol{Z}_M^T \boldsymbol{R}^l \boldsymbol{Z}_M \,\mathrm{d}z \right) \boldsymbol{B}_M \,\mathrm{d}x \tag{8}$$

where z and x denote the element coordinates in transverse and lateral directions, x_i and x_{i+1} are the nodes building the eth element, b is the width of the beam, and h_{i-1} is the distance from the lower surface of the kth sublaminate to the midplane of the beam, and h_i is the distance from the upper surface of the kth sublaminate to the midplane.

The integrations with respect to z can also be computed as

$$\int_{h_{i-1}}^{h_i} \boldsymbol{Z}_K^T \boldsymbol{Q}^l \boldsymbol{Z}_K \,\mathrm{d}z = \sum_{l=1}^{P_k+1} \int_{h_{i-1}^l}^{h_i^l} \boldsymbol{Z}_K^T \boldsymbol{Q}^l \boldsymbol{Z}_K \,\mathrm{d}z$$

$$\int_{h_{i-1}}^{h_i} \boldsymbol{Z}_M^T \boldsymbol{R}^l \boldsymbol{Z}_M \,\mathrm{d}z = \sum_{l=1}^{P_k+1} \int_{h_{i-1}^l}^{h_i^l} \boldsymbol{Z}_M^T \boldsymbol{R}^l \boldsymbol{Z}_M \,\mathrm{d}z \tag{9}$$

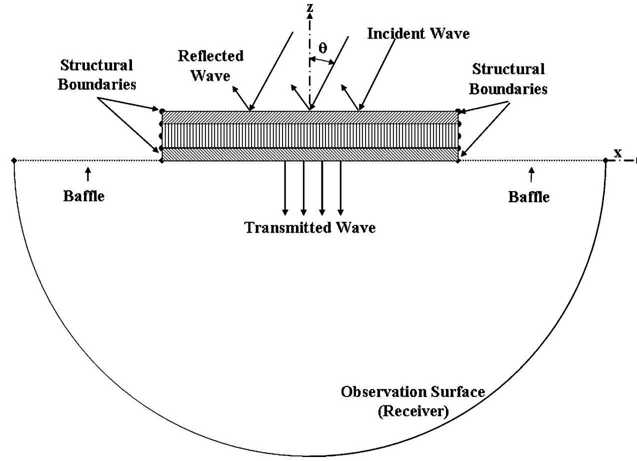

Fig. 1 Coordinate system of the infinitely baffled multilayered sandwich beam.

where h_{i-1}^l and h_i^l indicate the lower and upper surface distance of the lth layer from the global midsurface of the beam. Because the lth physical layer is a member of the kth sublaminate, $h_{i-1}^1 = h_{i-1}$ and $h_i^{P_k+1} = h_i$, where P_k is the number of physical layers in the kth sublaminate. When there is more than one physical layer in a sublaminate, the summation of all of the integrations from the lower to upper thickness coordinates of each physical layer gives the complete integration over the sublaminate.[12]

The assembly of element stiffness and mass matrices and nodal displacement vectors gives the global stiffness and mass matrices and global nodal displacement vector, which are denoted by $\boldsymbol{K}$, $\boldsymbol{M}$, and $\boldsymbol{u}$, respectively.

Assume that the multilayered beam is infinitely baffled as shown in Fig. 1. In this study, we neglect the reverse fluid loading on the bottom surface of the beam. Consider a plane acoustic wave of frequency ω that excites the top of the beam. The resultant acoustic pressure distribution on the beam as a function of lateral coordinate is given by

$$p_i(x, \omega) = p_i(x) e^{j\omega t} \tag{10}$$

where it is assumed that $p_i(x) = P \exp[jk\cos(\theta)x]$ in which k is the wave number of the sound wave, θ is the incident angle, and P is the predescribed amplitude of the acoustic pressure. The resultant nodal force vector in the transverse direction on the top surface can be calculated as a function of element lateral coordinate r:

$$\boldsymbol{f}_e(x) e^{j\omega t} = \left[\int_{x_i}^{x_{i+1}} p_i(x) \boldsymbol{h}^T(x) b \,\mathrm{d}x \right] e^{j\omega t} \tag{11}$$

where $\boldsymbol{h}(x)$ is a surface interpolation function along the x direction.

An assembly of all of the local force vectors leads to the global nodal force vector $\boldsymbol{f} e^{j\omega t}$. Further, we assume that the structural loss of the beam is characterized by a nodal damping matrix $\boldsymbol{C}$. The response of the system is harmonic $\boldsymbol{u} e^{j\omega t}$ satisfying the following equation:

$$[-\omega^2 \boldsymbol{M} + j\omega \boldsymbol{C} + \boldsymbol{K}]\boldsymbol{u} = \boldsymbol{f} \tag{12}$$

The boundary conditions of the sandwich beam can be imposed on $\boldsymbol{u}$ in the solution process. In the following analysis, we shall assume a Rayleigh damping such that $\boldsymbol{C} = \alpha \boldsymbol{K} + \beta \boldsymbol{M}$, where α and β are prespecified constants.

On the bottom surface of the beam in Fig. 1, the transmitted acoustic pressure $p_t(\boldsymbol{r}_{S'}) e^{j\omega t}$ at an receiver point $\boldsymbol{r}_{S'}$ because of the surface normal velocity $v(\boldsymbol{r}_S)$ can be written as

$$p_t(\boldsymbol{r}_{S'}) = \frac{i\omega\rho_a}{2\pi} \int_S v(\boldsymbol{r}_S) \frac{e^{-ikR}}{R} \,\mathrm{d}S \tag{13}$$

where ρ_a is the air density, $\boldsymbol{r}_S$ is the position vector of the surface element $\mathrm{d}S$ with the normal velocity $v(\boldsymbol{r}_S)$, S is the vibrating surface of the beam, and $R = |\boldsymbol{r}_S - \boldsymbol{r}_{S'}|$. Equation (13) is known as the Rayleigh integral. The acoustic power W radiated from the baffled beam is given by an integration over the receiver surface S':

$$W = \frac{1}{2}\int_{S'}\int_{S} v(\boldsymbol{r}_S)\left(\frac{\omega\rho_a}{2\pi}\frac{\sin(kR)}{R}\right)v^*(\boldsymbol{r}_{S'})\,\mathrm{d}S\,\mathrm{d}S' \tag{14}$$

where the asterisk indicates complex conjugate and $v^*(\boldsymbol{r}_{S'})$ is the normal velocity of the receiver surface of the beam at $\boldsymbol{r}_{S'}$.

When the receiver and source are on the surface of the beam, $\mathrm{d}S = b\,\mathrm{d}r_S$ and $\mathrm{d}S' = b\,\mathrm{d}r_{S'}$, and the discretization of the normal velocities on the receiver element e_k and source element e_j can be represented by an approximation:

$$v(r_S) = \boldsymbol{h}^T(r_S)\boldsymbol{v}_{e_j}, \qquad v(r_{S'}) = \boldsymbol{h}^T(r_{S'})\boldsymbol{v}_{e_k}$$

$$\boldsymbol{v}_{e_j}^T = [v_j \quad v_{j+1}], \qquad \boldsymbol{v}_{e_k}^T = [v_k \quad v_{k+1}] \tag{15}$$

where $\boldsymbol{h}(r_S)$ and $\boldsymbol{h}(r_{S'})$ are the interpolation vectors for source and receiver elements, j and $j+1$ are the nodes of the e_j^{th} source element, and k and $(k+1)$ denote the nodes of the e_k^{th} receiver element.

The substitution of Eq. (15) into Eq. (14) results in

$$W = \frac{\omega\rho_a b^2}{8\pi}\frac{1}{2}\sum_{j=1}^{n}\sum_{k=1}^{n}\boldsymbol{v}_{e_j} \times \int_{r_{e_k}}\int_{r_{e_j}}\frac{\sin(kR)}{R}\boldsymbol{h}(r_S)\boldsymbol{h}^T(r_{S'})\,\mathrm{d}r_S\,\mathrm{d}r_{S'}\cdot\boldsymbol{v}_{e_k}^* \equiv \frac{1}{2}\sum_{ej=1}^{n}\sum_{ek=1}^{n}\boldsymbol{v}_{e_j}^T\boldsymbol{B}_{jk}\boldsymbol{v}_{e_k}^* \tag{16}$$

where $R = |r_S - r_{S'}|$, n is the number of elements on the surface, and r_{e_j} and r_{e_k} are the source and receiver element boundaries. After the assembly of elemental matrices $\boldsymbol{B}_{jk}$ and nodal velocity vectors, a quadratic expression of the radiated acoustic power is obtained as

$$W = \tfrac{1}{2}\boldsymbol{v}^T\boldsymbol{B}\boldsymbol{v}^* \tag{17}$$

The radiated acoustic power is a function of design variables of geometric and material parameters. Let $\boldsymbol{x}^T = [x_1, x_2, \ldots, x_N]$ be a vector of N design variables. Hence, we can denote $W = W(\boldsymbol{x})$.

Optimization

To design a structure that radiates minimum acoustic power, we pose a constrained nonlinear optimization problem as follows.

Minimize:

$$f(\boldsymbol{x}) = W(\boldsymbol{x}) \qquad \boldsymbol{x} \in R^N \tag{18}$$

Subject to:

$$\boldsymbol{x}_{\mathrm{lb}} \le \boldsymbol{x} \le \boldsymbol{x}_{\mathrm{ub}} \tag{19}$$

$$g_i(\boldsymbol{x}) = 0 \qquad i = 1, \ldots, q \tag{20}$$

$$c_i(\boldsymbol{x}) \le 0 \qquad i = q+1, \ldots, p \tag{21}$$

where $f(\boldsymbol{x})$ is the objective function to be minimized with respect to the design variables $\boldsymbol{x}$. Here $\boldsymbol{x}_{\mathrm{lb}}$ and $\boldsymbol{x}_{\mathrm{ub}}$ denote the lower and upper bounds of the design variables, and $g_i(\boldsymbol{x})$ and $c_i(\boldsymbol{x})$ are equality and inequality constraints of the design variables.

An example of a set of the design variables is

$$\boldsymbol{x}^T = \left[t^1, \rho^1, Q_{jk}^1; \ldots t^l, \rho^l, Q_{jk}^l; \ldots\right] \tag{22}$$

where the superscripts refer to a physical layer of the laminate, t^l is the thickness, ρ^l is the mass density, and Q_{jk}^l is the (jk)th component of the stiffness matrix of the physical layer. The maximum allowable thickness t_0 of the beam, the overall mass m_0, and the smallest allowable fundamental frequency ω_0 of the structure can be employed as the constraints for the optimization problem

$$\sum_{l=1}^{P} t^l \le t_0 \tag{23}$$

$$bL\sum_{l=1}^{P} t^l\rho^l \le m_0 \tag{24}$$

$$\omega_1(\boldsymbol{x}) \ge \omega_0 \tag{25}$$

where P stands for the total number of physical layers and $\omega_1(\boldsymbol{x})$ denotes the fundamental frequency of the structure.

We apply a pattern search technique to solve the optimization problem subject to linear and nonlinear constraints. This search technique is a subset of direct search methods.[19,20] The pattern search algorithm looks for the optimum by making two sequential moves. One is called the exploratory move and the other the pattern move. The first move explores the local behavior of the objective function to form the pattern, and the second establishes a global step size in the identified pattern direction.

In the present application, we have nonlinear constraints given by Eqs. (24) and (25). To take advantage of the fact that the pattern search algorithm does not compute derivatives of the objective function, we can impose these nonlinear constraints by including them as part of the objective function. An example of the extended objective function is given by

$$f(\boldsymbol{x}) = \begin{cases} \gamma, & \text{if} \quad bL\sum_{l=1}^{P} t^l\rho^l > m_0 \\ \gamma, & \text{if} \quad \omega_1(\boldsymbol{x}) < \omega_0 \\ W(\boldsymbol{x}), & \text{otherwise} \end{cases} \tag{26}$$

where $\gamma > 0$ is a sufficiently large number to reject the design parameters that violate the nonlinear constraints.

Inclusion of the nonlinear constraints into the objective function provides a way to streamline the programing and allows us to increase the computational efficiency because the nonlinear constraints, particularly the fundamental frequency constraint, are already computed during the process of obtaining the radiated acoustic power $W(\boldsymbol{x})$. As a result, imposing these nonlinear constraints does not add additional computational burden with the current approach.

Numerical Results

Consider a simply supported sandwich beam 2 m long and 0.025 m wide. The geometrical and material properties of the baseline beam define the initial condition of the optimization problem. The top and bottom skins of the baseline beam are assumed to be identical and made of graphite epoxy. The stiffness components and the mass density for the skins are

$$Q_{11}^s = 1.67\times10^{10}\ \mathrm{Pa}, \qquad Q_{12}^s = 5.00\times10^{9}\ \mathrm{Pa}$$

$$Q_{22}^s = 1.08\times10^{10}\ \mathrm{Pa}, \qquad Q_{33}^s = 6.40\times10^{9}\ \mathrm{Pa}$$

$$\rho^s = 1760\ \mathrm{kg/m^3} \tag{27}$$

The core material is Klegecell foam. The stiffness components and the mass density of the core are

$$Q_{11}^c = 1.30\times10^{8}\ \mathrm{Pa}, \qquad Q_{12}^c = 5.20\times10^{7}\ \mathrm{Pa}$$

$$Q_{22}^c = 0.80\times10^{8}\ \mathrm{Pa}, \qquad Q_{33}^c = 5.00\times10^{7}\ \mathrm{Pa}$$

$$\rho^c = 130\ \mathrm{kg/m^3} \tag{28}$$

The Rayleigh damping coefficients α and β are chosen to be 0.001 for all layers just to avoid the resonant responses. The thicknesses of the lower skin, core, and upper skin of the initial beam are 0.01, 0.2, and 0.01 m, respectively. The thickness-to-length aspect ratio of the beam is 11/100. The top surface of the beam is excited by a plane wave acoustic pressure with a 60-deg incident angle θ at 450 Hz, and the magnitude of the resultant acoustic pressure is 1×10^3 Pa. The beam is discretized by 30 longitudinal $\times$ 3 sublaminate elements, which are constituted by the linear shape functions in both lateral and transverse directions.

The stiffness components Q_{11}, Q_{12}, and Q_{22} of all three layers are considered as the design parameters to minimize the objective function in Eq. (18). The lower and upper bounds of the design parameters are fixed by $\frac{1}{4}$ and four times the initial values. The minimum fundamental frequency is bounded by the fundamental frequency of the baseline beam. Also, the positive definiteness of the modulus matrix $\boldsymbol{Q}$ is imposed. Note that this beam is uniform along both the length and the depth.

The optimum stiffness components scaled by the corresponding values of the baseline beam are given in Fig. 2. The acoustic intensities of the baseline and optimized beams are plotted in Fig. 3. The acoustic power computed from the areas under the intensity curves are 10.45×10^{-5} and 5.90×10^{-5} W, respectively. The reduction corresponds to 2.50 dB. An acoustic-power-level (APL) index is defined to determine the improvement by the optimized beam relative to the initial beam:

$$\mathrm{APL} = 10 \times \log_{10}(W/W_{\mathrm{ref}}) \tag{29}$$

where W is the acoustic power radiated from the beam and W_{ref} is a reference power level that is the radiating surface area times 10^{-12} W/m^2 for the air. In addition, an acoustic transmission loss (ATL) is introduced to evaluate the acoustic power transmitted through the beam:

$$\mathrm{ATL} = 10 \times \log_{10}\left(\frac{1}{2} Re \int_0^L p_{\mathrm{net}} v_t^* b \,\mathrm{d}x \bigg/ W\right) \tag{30}$$

where v_t is the normal velocity of the top surface where the excitation is applied. APL and ATL as a function of frequency are shown in Fig. 4.

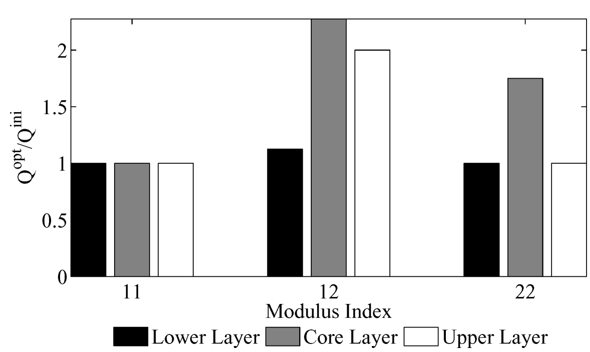

Fig. 2 Optimum modulus components of the uniform beam scaled by those of baseline beam.

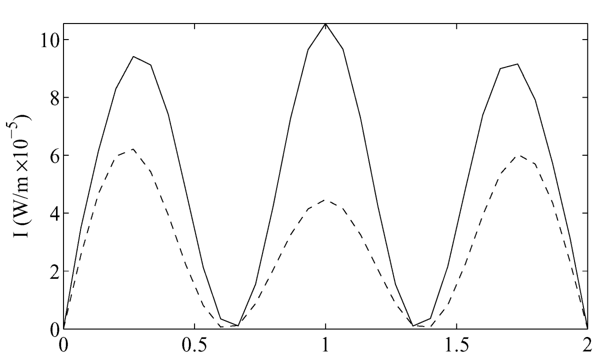

Fig. 3 Acoustic intensity distribution along the beams: ——, baseline beam and - - - -, optimized uniform beam.

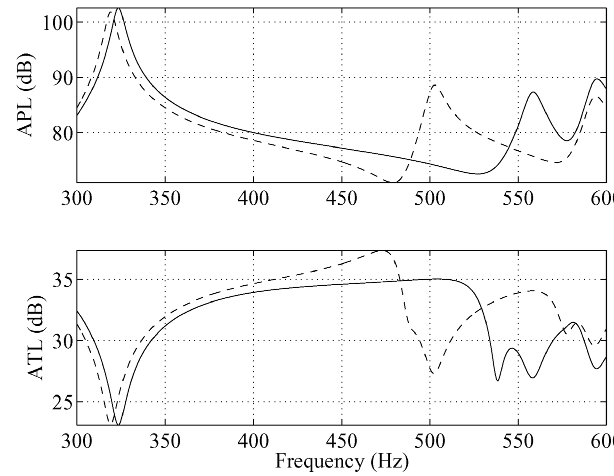

Fig. 4 APL and ATL of the beams as a function of frequency: ——, baseline beam and - - - -, optimized nonuniform beam.

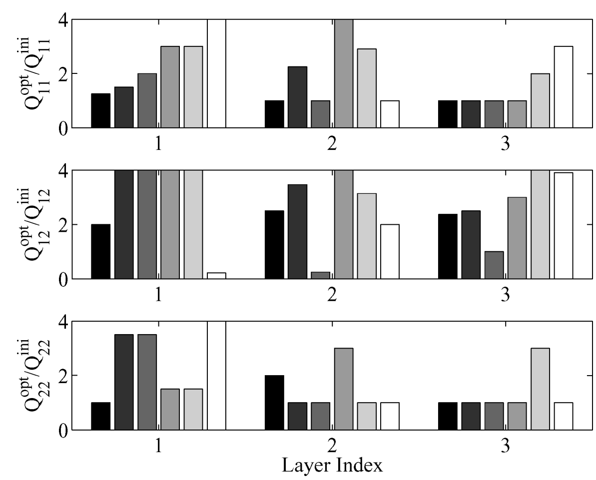

Fig. 5 Optimum modulus components of the nonuniform beam scaled by those of baseline beam. Each layer has six subsections arranged from the left (black bar) to the right (white bar) in the chart.

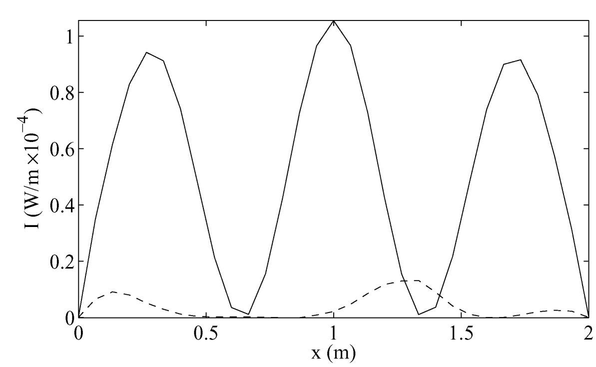

Fig. 6 Acoustic intensity distribution along the beams: ——, baseline beam and - - - -, optimized nonuniform beam.

We have extended this study to nonuniform sandwich beams. The beam is divided into six segments. In each segment, the design variables of the layers are uniform. The baseline uniform beam is optimized under the same constraints. Figure 5 shows optimum design variables that are scaled by the corresponding baseline beam values. The results are compared with the optimized uniform beam. Figure 6 shows the intensity distributions for baseline beam and optimized nonuniform beam. The acoustic power of the nonuniform beam is reduced to 0.75×10^{-5} W at 450 Hz, which increases the reduction of the power up to 11.45 dB. APL and ATL of the

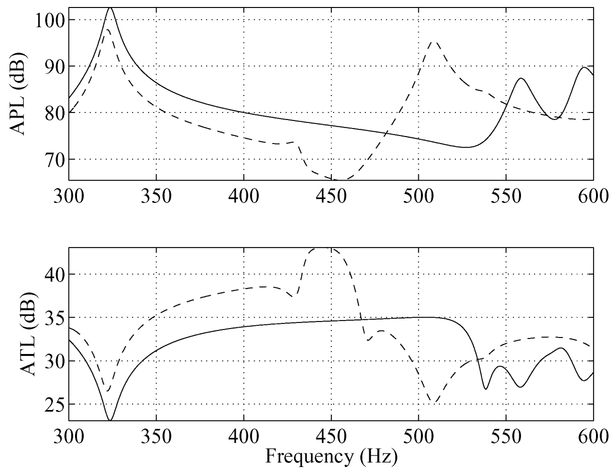

Fig. 7 APL and ATL of the beams as a function of frequency: ——, baseline beam and - - - -, optimized nonuniform beam.

optimized nonuniform beam are much improved as compared to the baseline beam over a wider range of frequencies, as shown in Fig. 7. The acoustic transmission loss is improved more than the acoustic power level by means of nonuniformity in the design parameters along the beam.

The solution to the equation of motion helps us better understand the improvement stemming from nonuniformity:

$$\boldsymbol{u} = \boldsymbol{\Phi}[\boldsymbol{\Lambda} - \omega^2 \boldsymbol{I}]^{-1} \boldsymbol{\Phi}^H \boldsymbol{f} \tag{31}$$

where $\boldsymbol{\Phi}$ and $\boldsymbol{\Lambda}$ are the eigenvector and diagonal eigenvalue matrices of the stiffness and mass matrices $\boldsymbol{K}$ and $\boldsymbol{M}$ and the superscript H denotes Hermitian transpose. The design parameters of the uniform beam are only able to reorganize the natural frequencies and cannot change much the mode shapes of the beam response, whereas design parameters of the nonuniform beam can significantly change both mode shapes and natural frequencies of the system. Hence, the design parameters can not only improve the radiation characteristics of the modes, but also reduce the work done by the loading on the system described by the terms such as $\phi_i^T \boldsymbol{f}$, where ϕ_i is the ith modal vector of the system.

Conclusions

We have presented a structural-acoustic optimization study of multilayered sandwich beams with anisotropic material properties. The objective of optimization is to minimize the radiated acoustic power from the beam excited by a planar acoustic wave. The design variables of the example are the components of the elastic modulus matrix. Significant reduction of the sound radiation can be achieved with the optimized multilayered beam as compared with the baseline beam. Furthermore, we have found that the nonuniform multilayered beam with more independent design variables for optimization can have much higher reduction in sound radiation than the uniform beam with less independent design variables.

Acknowledgment

This research is supported by a grant (CMS-0219217) from the National Science Foundation.

References

[1]Belegundu, A. D., Salagame, R. R., and Koopmann, G. H., "General Optimization Strategy for Sound Power Minimization," *Structural Optimization*, Vol. 8, No. 2–3, 1994, pp. 113–119.

[2]Koopmann, G. H., and Fahnline, J. B., "Minimizing Sound Power Using Material Tailoring," *Designing Quiet Structures*, Academic Press, San Diego, CA, 1997, pp. 145–175.

[3]Tinnsten, M., "Optimization of Acoustic Response—A Numerical and Experimental Comparison," *Structural and Multidisciplinary Optimization*, Vol. 19, No. 2, 2000, pp. 122–129.

[4]Thamburaj, P., and Sun, J. Q., "Optimization of Anisotropic Sandwich Beams for Higher Sound Transmission Loss," *Journal of Sound and Vibration*, Vol. 254, No. 1, 2002, pp. 23–36.

[5]Thamburaj, P., "Structural-Acoustic Studies of Sandwich Structures for Global Transport Aircraft," Ph.D. Dissertation, Dept. of Mechanical Engineering, Univ. of Delaware, Newark, DE, 2001.

[6]Cunefare, K. A., "The Minimum Multimodal Radiation Efficiency of Baffled Finite Beams," *Journal of the Acoustical Society of America*, Vol. 90, No. 5, 1991, pp. 2521–2529.

[7]Naghshineh, K., Koopmann, G. H., and Belegundu, A. D., "Material Tailoring of Structures to Achieve a Minimum Radiation Condition," *Journal of the Acoustical Society of America*, Vol. 92, No. 2, 1992, pp. 841–855.

[8]Denli, H., Frangakis, S., and Sun, J. Q., "Normalizations in Acoustic Optimization with Rayleigh Integral," *Journal of Sound and Vibration*, Vol. 284, No. 3–5, 2005, pp. 1229–1238.

[9]Elbeyli, O., Thamburaj, P., and Sun, J. Q., "Structural-Acoustic Studies of Sandwich Structures: A Review," *Shock and Vibration Digest*, Vol. 33, No. 5, 2001, pp. 372–384.

[10]Wang, T., Sokolinsky, V. S., Rajaram, S., and Nutt, S. R., "Assessment of Sandwich Models for the Prediction of Sound Transmission Loss in Unidirectional Sandwich Panels," *Applied Acoustics*, Vol. 66, No. 3, 2005, pp. 245–262.

[11]Noor, A. K., Burton, W. S., and Bert, C. W., "Computational Models for Sandwich Panels and Shells," *Applied Mechanics Reviews*, Vol. 49, No. 3, 1996, pp. 155–199.

[12]Reddy, J. N., "Layerwise Theory and Variable Kinematic Models," *Mechanics of Laminated Composite Plates: Theory and Analysis*, CRC Press, Boca Raton, FL, 1997, pp. 725–816.

[13]Lewis, R. M., Torczon, V., and Trosset, M. W., "Direct Search Methods: Then and Now," *Journal of Computational and Applied Mathematics*, Vol. 124, No. 1–2, 2000, pp. 191–207.

[14]Kant, T., and Swaminathan, K., "Estimation of Transverse/Interlaminar Stresses in Laminated Composites—A Selective Review and Survey of Current Developments," *Composite Structures*, Vol. 49, No. 1, 2000, pp. 65–75.

[15]Reddy, J. N., "An Evaluation of Equivalent-Single-Layer and Layerwise Theories of Composite Laminates," *Composite Structures*, Vol. 25, No. 1–4, 1993, pp. 21–35.

[16]Nosier, A., Kapania, R. K., and Reddy, J. N., "Free Vibration Analysis of Laminated Plates Using a Layerwise Theory," *AIAA Journal*, Vol. 31, No. 12, 1993, pp. 2335–2346.

[17]Wu, C. P., and Chen, W. Y., "Vibration and Stability of Laminated Plates Based on a Local High Order Plate Theory," *Journal of Sound and Vibration*, Vol. 177, No. 4, 1994, pp. 503–520.

[18]Gaudenzi, P., Barboni, R., and Mannini, A., "A Finite Element Evaluation of Single-Layer and Multi-Layer Theories for the Analysis of Laminated Plates," *Composite Structures*, Vol. 30, No. 4, 1995, pp. 427–440.

[19]Torczon, V., "On the Convergence of Pattern Search Algorithms," *SIAM Journal on Optimization*, Vol. 7, No. 1, 1997, pp. 1–25.

[20]Lewis, R. M., and Torczon, V., "Pattern Search Algorithms for Bound Constrained Minimization," *SIAM Journal on Optimization*, Vol. 9, No. 4, 1999, pp. 1082–1099.

A. Palazotto
Associate Editor